Available online at www.sciencedirect.com
ScienceDirect
Journal of the European Ceramic Society 31 (2011) 2155–2165
www.elsevier.com/locate/jeurceramsoc

SiC-based refractory paints prepared with alkali aluminosilicate binders

V. Medri [a,*], S. Fabbri [a], A. Ruffini [a], J. Dedecek [b], A. Vaccari [c]

[a] CNR-ISTEC, Via Granarolo 64, 48018 Faenza, Italy
[b] J. Heyrovsky Institute of Physical Chemistry, Academy of Sciences of the Czech Republic, Dolejskova 2155/3, 18 223, Prague 8, Czech Republic
[c] Dipartimento di Chimica Industriale e dei Materiali, Alma Mater Studiorum – Università di Bologna, Viale Risorgimento 4, 40136, Bologna, Italy

Received 8 February 2011; received in revised form 19 April 2011; accepted 5 May 2011
Available online 31 May 2011

Abstract

Refractory paints based on silicon carbide (SiC) were developed using inorganic alkali aluminosilicates binders. In order to optimize the binders, different raw materials have been tested for their preparations (calcined kaolin, commercial metakaolin, α-alumina and fumed silica synthetic powders). The alkali activator was an aqueous solution of KOH/K_2SiO_3. The SiO_2:Al_2O_3 molar ratio was equal to 4 and the SiO_2:K_2O molar ratio was 2. Calcined kaolin and metakaolin in alkaline conditions dissolved and re-precipitated to form geopolymer resins acting as a glue for the un-reacted Al–Si materials and SiC (90 wt.%). Binders based on α-alumina and fumed silica behaved as water glass. Binders and SiC paints were tested and characterized in inert and oxidative atmospheres up to 1300 °C. The oxidation of the SiC paints was 50% lower than that of pure SiC, evidencing a key role of the alkali aluminosilicate binders during the thermal treatments.

Keywords: C. Corrosion; C. Thermal properties; D. SiC; D. Silicate; Geopolymers

1. Introduction

High-temperature resistant coatings represent an important issue due to their relevant potential applications (turbines, engines, aeronautic, etc.). Although many ceramic coatings applied with several technologies have been developed, their preparation is expensive, complex and needs specific equipments.[1–6] Ceramic coatings may also be formed by spray, dip, or brush ceramic paint directly on the surface of the components. This represents an effective, economic, and workable way of protecting metal or ceramic components in severe environments. However, the preparation of a high-temperature resistant ceramic paint requires the application of inorganic binders.[7] Binders based on inorganic compounds exhibit significant advantages, since they are non-off gassing during setting and do not burn, ignite or release any smoke or gas when heated.

Alkali aluminosilicate binders may be regarded as inorganic polymers, the so called geopolymers, and represent promising inorganic alternatives to organic matrices for the preparation of composite materials.[8,9] Geopolymers belong to alkali bonded ceramics (ABC),[10] i.e. one class of the chemically bonded ceramics (CBCs). Chemically bonded ceramics can be produced at low temperatures by chemical reactions. The reaction of an aluminosilicate powder with a highly concentrated alkali hydroxide solution (KOH, NaOH) as an activator and/or with silicate (potassium or sodium) solution results in the formation of a synthetic alkali aluminosilicate. This material can be either amorphous or semi-crystalline. Nevertheless, recent researches suggest that geopolymers may be regarded as an amorphous analogue of zeolites.[11,12] During geopolymerization a three-dimension (3-D) network consisting of SiO_4^{2-} and AlO^{4-} tetrahedra sharing oxygen corners and linked in an alternating sequence is formed. The geopolymer resin consists of nano-precipitates[11,13] that act like a glue sticking together the unreacted Al–Si starting materials and fillers (powders or fibres, glasses, ceramics, metals or organics) forming the geopolymer composite materials. Different fillers can be used to tailor specific physical and thermo-mechanical properties of the geopolymer composites in the dependence on their applications.[14–22]

Metakaolin and industrial wastes such as fly ashes are predominantly used as starting raw aluminosilacate powders. However, also natural minerals, blast-furnace slags or any source

* Corresponding author. Tel.: +39 0546699751; fax: +39 054646381.
E-mail addresses: valentina.medri@istec.cnr.it, valentinamedri@hotmail.com (V. Medri).

0955-2219/$ – see front matter © 2011 Elsevier Ltd. All rights reserved.
doi:10.1016/j.jeurceramsoc.2011.05.006

Table 1
Characteristics of the natural aluminosilicatic raw powders. LOI: loss of ignition at 1000 °C; D50: mean grain size; ssa: specific surface area.

Sample	Chemical composition, %								LOI	D50	ssa	Crystalline phases
	Al_2O_3	SiO_2	Fe_2O_3	TiO_2	K_2O	Na_2O	CaO	MgO	%	μm	m^2/g	
Kaolin source for metakaolin A	37.60	43.73	1.23	1.65	0.51	0.21	0.15	0.20	14.7	1.2 3.5[a]	18 30[a]	Quartz TiO_2 Gibsite[b] Illite 2M2
Metakaolin B	39.71	53.55	1.50	1.40	0.92	0.00	0.09	0.15	2.7	1.7	19	QuartzMuscovite 3T

[a] After calcination at 750 °C for 15 h.
[b] Gibbsite transformed into γ-Al_2O_3 during calcination.

of silica and alumina can be employed. Nevertheless, metakaolin remains the most reactive under alkaline conditions.[23]

The treatment of geopolymers at elevated temperatures results in their transformation to glass-ceramics. Depending on the stoichiometry and composition of starting material, the formation of nepheline ($Na_2O{\cdot}Al_2O_3{\cdot}2SiO_2$, $T_{melt} > 1526$ °C), leucite ($K_2O{\cdot}Al_2O_3{\cdot}4SiO_2$ $T_{melt} > 1698$ °C), and pollucite ($Cs_2O{\cdot}Al_2O_3{\cdot}4SiO_2$, $T_{melt} > 1900$ °C) has been previously reported.[10,19,24,25]

In this study, the fabrication of an easy-to-prepare (by mixing of two components) and easy-to-apply (by brushing) SiC refractory coating based on geopolymer binder is reported. A coarse re-crystallized α-SiC (R-SiC) was used as the main filler component of the refractory paint. Ability to withstand high working temperatures, excellent corrosion resistance, good thermal shock resistance and high thermal conductivity are typical properties of R-SiC. The alkali aluminosilicate binders were prepared using either metakaolins or α-alumina and fumed silica as raw source materials and alkali aqueous solution of KOH/K_2SiO_3 as activator. Pure binders and prepared SiC paints were tested and characterized in inert and oxidative atmospheres up to 1300 °C.

2. Experimental procedure

2.1. Binders and paints preparation

Three alkali aluminosilicate binders were prepared by using two different metakaolins and α-alumina and fumed silica as raw materials. Metakaolin A was prepared from commercial kaolin (BS4, AGS Mineraux, Clèrac, France) by calcination at 750 °C for 15 h in an electric kiln. Metakaolin B was M1200S always from AGS Mineraux. The main characteristics of these two parent materials are reported in Table 1. BET analyses were performed using a SORPTY 1750 Carlo Erba Instrument. A Varian Liberty 200 inductively coupled plasma optical emission spectrometer (ICP-OES) was used for the composition analysis, Bruker D8 Advance diffractometer with CuKα radiation was used to analyze the crystalline phases.

As synthetic aluminosilicate sources, α-Al_2O_3 (Baykalox Alumina High Purity CR30F, Baykowsky, France) with a specific surface area of 26 m^2/g and fumed silica powder (99.8%, Sigma–Aldrich, Germany) with 255 m^2/g of specific surface area were used.

Potassium silicate solutions with a SiO_2:K_2O molar ratio equal to 2.00 and a H_2O:K_2O molar ratio equal to 23.00 were prepared by dissolving KOH pellets (purity >99%, Merck, Germany) into potassium silicate aqueous solution with a SiO_2:K_2O molar ratio equal to 3.57 (KSil 35Bè R3.5, Ingessil, Italy) under magnetic stirring. Geopolymer binder resins with SiO_2:Al_2O_3 molar ratio equal to 4.00 were prepared by manually mixing raw powders with the KOH/K_2SiO_3 aqueous solution. The resulting slurries were then placed in sealed plastic moulds and cured in a heater at 80 °C for 24 h.

Re-crystallized silicon carbide powder (R-SiC) (α-SiC grade 100F, SIKA TECH, Saint-Gobain Ceramic Materials, Germany) was used as a basic component of the paints. R-SiC powder exhibits a bi-modal distribution centred at 150 μm (20%) and 45 μm (80%), with a specific surface area of 0.58 m^2/g. Paints were prepared by eccentric mixing of the R-SiC (65 wt.%) with metakaolins or α-Al_2O_3 and fumed silica (7 wt.%) followed by mixing of the powder mixture with the KOH/K_2SiO_3 solution (14 wt.%) and additional water (14 wt.%) with spatula. After setting and water removal, the weight fraction of R-SiC corresponded to 90% of the paint.

Paints were placed in sealed plastic moulds to produce cylinders of 25 mm length and 5 mm diameter or applied by brushing on Si_3N_4-TiN ceramic substrates (CTE 5×10^{-6} °C^{-1}) and cured at 80 °C for 24 h.

2.2. Microstructural characterization

Metakaolins were investigated by[27] Al MAS-NMR spectroscopy using a Bruker Avance 500 MHz (11.7 T) Wide Bore spectrometer, equipped with a 4 mm o.d. ZrO_2 rotor with a rotation speed of 12 kHz. High-power decoupling sequences with π/12 (0.7 μs) excitation pulse were applied to allow the quantitative analysis of the investigated samples. The[27] Al NMR observed chemical shift was referred to an aqueous solution of $Al(NO_3)_3$. For detailed and quantitative analyses, spectra were simulated using Dmfit software.[26]

Both binders and paints were examined after curing and thermal treatments by SEM-EDS (SEM, Cambridge S360, UK; EDS, INCA Energy 300, Oxford Instruments, UK) and XRD.

2.3. Thermal characterization and oxidation behaviour

Dilatometric analyses were performed with a DIL402 dilatometer (NETSCH, Geraetebau, Germany) on cylinders of

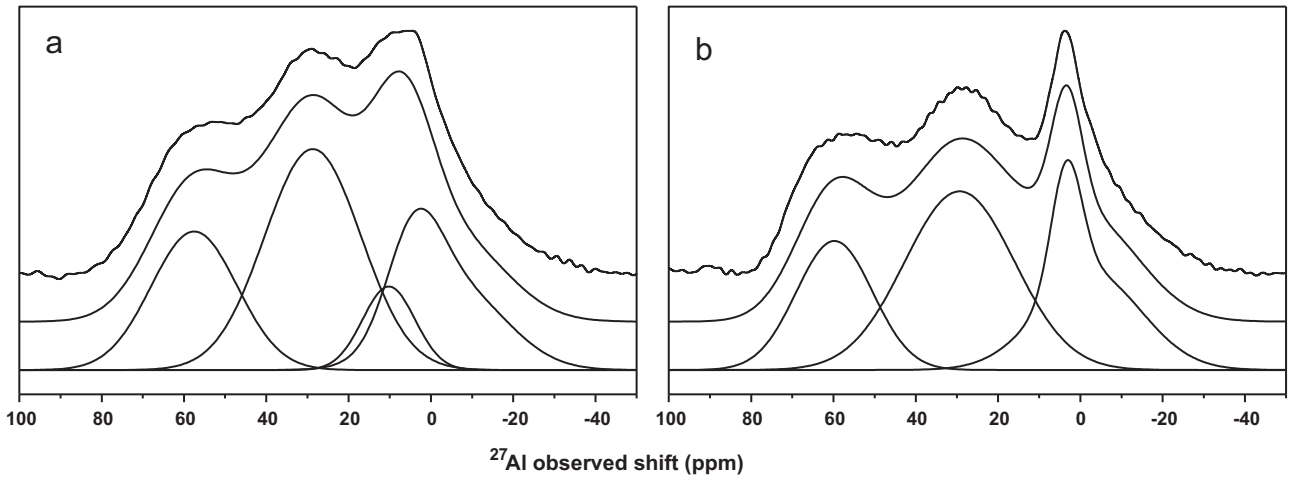

Fig. 1. Al single pulse MAS-NMR spectra of the metakaolins A (a) and B (b) with spectra simulations.[27]

25 mm length and 5 mm diameter up to 1300 °C in flowing Ar (heating rate 10 °C/min). Thermal treatments were performed both on binders and paints at 1300 °C under an Ar flux with a permanence of 1 h (heating rate 10 °C/min). The linear shrinkages were measured with a calliper (accuracy ±0.01 mm). Oxidation tests were performed on paints and R-SiC powder with a non-isothermal simultaneous thermal analysis (Polymer Thermal Science STA 1500) in static air with a heating rate of 10 °C/min. Long term oxidation tests were performed for 100 h at 1200 °C using a laboratory kiln and operating in static air.

2.4. Scratch tests

Adhesion of coatings to the substrate was evaluated before and after long term oxidation by a CSM Revetest apparatus, equipped with detectors for the acoustic emission (AE) and the frictional force (Fμ). The scratch test was performed with a moving diamond indenter pressed on the sample surface with increasing load (maximum applicable load 200 N). A diamond Rockwell C-like conic scratching tip with a 200 μm radius was used and the applied normal load was continuously increased up to 50 N, using a loading rate of 100 N/min and a speed of 10 mm/min. The normal load, friction force and acoustic emission signals were continuously recorded during scratching. The critical normal load for crack initiation, first cohesive failure and first exposure of the substrate material were determined by the changes in AE and/or Fμ reading, as well as by after-test optical and scanning electron microscopy examinations.

The mean surface roughness (R_a) of R-SiC coatings was reduced to a value lower than 10 μm by polishing the samples with diamond pastes. Further polishing was not possible to prevent the coating removal from the surface. It is known that a proper assessment of adhesion properties requires a lower surface roughness[27]; however, the experimental results obtained in the aforementioned conditions can be used as a qualitative comparison between the materials. Moreover, their repeatability gave confidence on their reliability as it will be seen below.

3. Results and discussion

3.1. Alkali aluminosilicate binders and SiC based paint

Metakaolin powders react in alkali medium giving geopolymer nano-precipitates that act as a binder of R-SiC powder. However, the metakaolin reactivity is not uniform and depends on both its morphology and degree of dehydroxylation, and may result in the different degrees of its geopolymerization.[28,29] The resulting un-reacted metakaolin then plays the role of filler, often improving mechanical properties of geopolymer formed.

The higher surface area of the calcined metakaolin A with respect to metakaolin B (Table 1) suggests a potentially higher reactivity during the initial dissolution process of geopolymerization. Moreover, the two parent metakaolins exhibit also different compositions in the term of crystalline phases inert to geopolymerization (Table 1). According to Zibouche et al.[30], the presence of inert secondary phases does not influence the geopolymerization reaction.

In both metakaolins,[27] Al MAS-NMR spectroscopy was employed to analyze the amount of aluminium atoms with different reactivity in the geopolymerization process. Single pulse[27] Al MAS-NMR spectra of both metakaolins together with their simulations are showed in Fig. 1. According to the literature,[29,31,32] the presence of octahedral (Al_{VI}), penta-coordinated (Al_V), and tetrahedral (Al_{IV}) Al atoms in oxidic environment is evidenced by resonances around 0, 30 and 60 ppm for both samples. Nevertheless, the two metakaolins differ in the intensity of the signal of Al_{IV} and Al_V atoms. Moreover, in the spectrum of metakaolin A two signals in the octahedral region are present. The first, asymmetric and with a maximum at 3 ppm, was also observed in metakaolin B. The resonance at 10 ppm can be instead attributed to illite or γ-Al_2O_3 and reflects the presence of impurities in the raw material. This suggestion is in a good agreement with the results of X-ray diffraction (Table 1). Al_V and Al_{IV} atoms are formed during the dehydroxylation of the kaolinite to form metakaolinite and the Al_V atoms have been reported to be most reactive in alkaline conditions.[29] Quantitative analysis of the spectra evidences the presence of

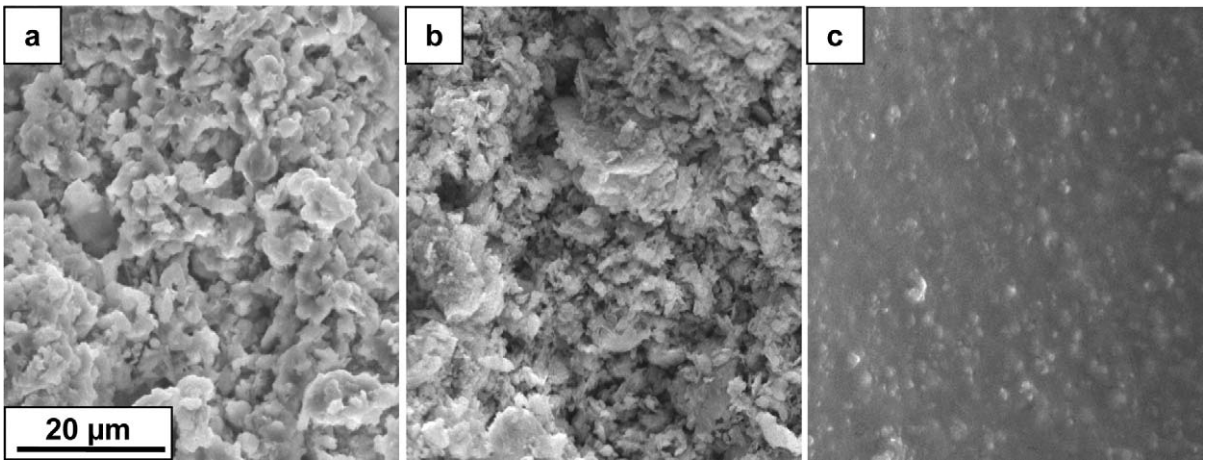

Fig. 2. SEM micrographs showing the microstructure of the alkali aluminosilicate binders after curing. The raw powders are metakaolins A (a) or B (b), and α-Al_2O_3 plus fumed silica (c).

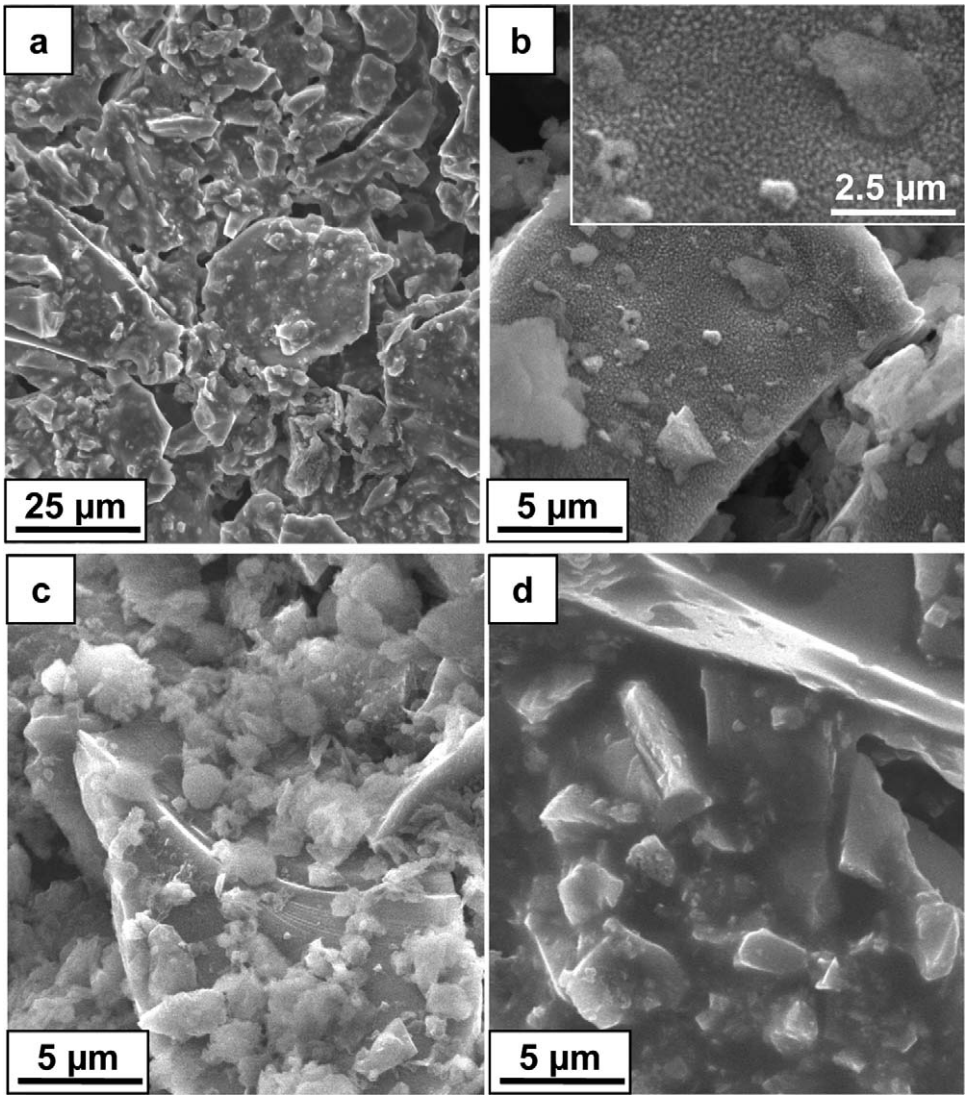

Fig. 3. SEM micrographs showing the microstructure of the surface (a) and of the bulk (b)–(d) of the R-SiC-based paints after setting. The aluminosilicate raw powders are metakaolin A (a) and (b), metakaolin B (c) and α-Al_2O_3 plus fumed silica (d).

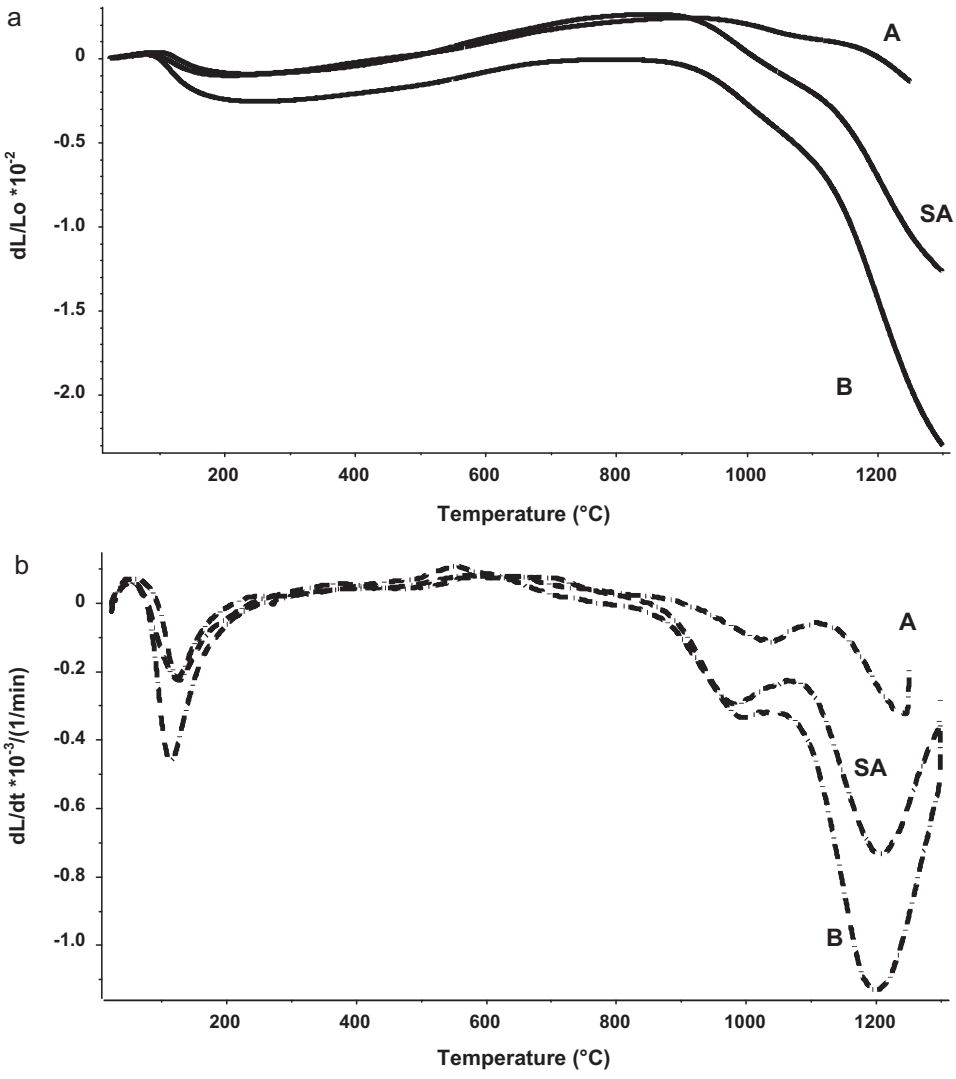

Fig. 4. Dilatometric analyses of R-SiC-based paints from the different aluminosilicate raw powders (a) and the derivatives of the dilatometric plots (b). SA stands for synthetic raw materials, i.e. α-Al_2O_3 plus fumed SiO_2.

40% of Al_V in metakaolin A compared to 50% in metakaolin B; on the other side, concentration of Al_{VI} is higher in metakaolin B compared to metakaolin A (25 and 20%, respectively).

SEM micrographs of the fracture surfaces of the alkali aluminosilicate resins after setting are reported in Fig. 2. Binder resin prepared using BS4 (Fig. 2a) exhibits both larger grain size and tighter bond between particles than the resin obtained from M1200S (Fig. 2b), where unreacted potassium silicate was clearly detected.[28] The microstructure of the binder synthesised using α-alumina and fumed silica was continuous, due to the solidification of the water glass (potassium silicate solution) embedding unreacted Al_2O_3 particles (Fig. 2c).

The microstructure of the surfaces appears almost the same in all paints, because of a water glass enrichment on the top layer (Fig. 3a). However, according to the previously mentioned features, R-SiC grains are covered by geopolymer precipitates of about 70 nm when metakaolin A is used (Fig. 3b) or by partially reacted particles when metakaolin B is used (Fig. 3c). On the contrary, R-SiC is surrounded and embedded by a layer of water glass in the case of binder prepared using α-alumina and fumed silica (Fig. 3d).

3.2. Thermal behaviour in inert atmosphere

The thermal behaviour of the prepared paints was monitored by dilatometric analysis up to 1300 °C in Ar (Fig. 4); the inert atmosphere was chosen to avoid to increase the amount of silica in the system due to R-SiC oxidation at high temperature.

The derivatives of the dilatometric plots (Fig. 4b) evidence the changes in axial shrinkages. The first contraction occurring in the temperature range 100–200 °C is related to the overall desorption of water from the micro and macro pores as already observed in geopolymers by Bell et al.[25] For all samples, the maximum rate of contraction is observed at 125 °C. Then, the plots exhibit an almost linear trend up to about 700 °C. In the temperature range 300–500 °C, the thermal expansion coefficients (CTE) are 5.7 and 4.8 and $5.2 \times 10^{-6}\,°C^{-1}$, respectively for paints where metakaolin A, metakaolin B and α-alumina

Table 2
Linear shrinkages of the binders and R-SiC paints after thermal treatment at 1300 °C for 1 h in Ar.

Aluminosilicatic raw powders	Linear shrinkage (%)	
	Resins	SiC paints
Metakaolin A	7.5	0.1
Metakaolin B	24.8	1.5
α-Al_2O_3; fumed SiO_2	melt	0.2

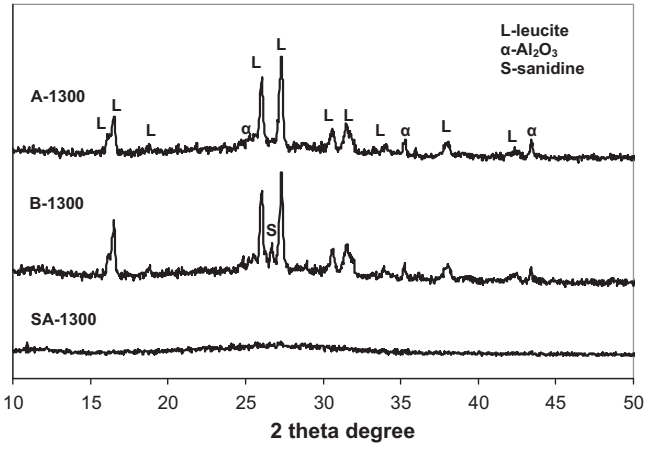

Fig. 5. XRD alkali aluminosilicate binders from the different raw powders after thermal treatment at 1300 °C for 1 h. SA stands for synthetic raw materials, i.e. α-Al_2O_3 plus fumed SiO_2, while 1300 indicates the temperature of the thermal treatment.

and fumed silica are used. These CTE values are close to R-SiC value (5–5.5 × 10^{-6} °C^{-1})[33] as a consequence of the rule of the mixtures.

Table 2 reports the shrinkages of the resin and paints after thermal treatment in Ar at 1300 °C for 1 h. The XRD spectra (Fig. 5) reveal the presence of leucite, as the main phase. Traces of α-Al_2O_3 are observed in the resin from metakaolin A, as the result of the γ- to α-Al_2O_3 phase transformation at high temperature. The high temperature form of sanidine (KSi_3AlO_8) is present in the resin from metakaolin B. Sanidine was also observed after multiple firings by Mackert and Evans.[34] In particular, the presence of sanidine may be attributed to an incongruent melting to leucite plus liquid above 1050 °C.[35] Moreover, the linear shrinkage after thermal treatment is about three times greater in the resin from metakaolin B than in the resin from metakaolin A (Table 2). The resin from α-alumina and fumed silica behaves as a glass in the system K_2O–Al_2O_3–SiO_2, giving a fully amorphous XRD pattern. However, the paint shrinkage is almost the same of the paint from metakaolin A. The alkali aluminosilicate binder from α-alumina and fumed silica exhibits the behaviour of water glass, allowing a better R-SiC particle packing, with a consequent low shrinkage due to particles rearrangement by heating.

Geopolymers with molar ratio SiO_2:Al_2O_3 equal to 4.00 have been shown to crystallize into leucite, $K_2O{\cdot}Al_2O_3{\cdot}4SiO_2$, by heating.[25] Moreover, compositional heterogeneities, together with the presence of free alkali ions in the geopolymer structure, favour the formation of a glassy phase.[25] Actually, the resins react only partially and metakaolin particles and potassium silicate are still present. This induces glass formation and a linear shrinkage that is proportional to the glass amount and viscosity during liquid phase sintering.[25] From dilatometric analyses and shrinkages after thermal treatments at 1300 °C, it may be concluded that the higher viscous flow is produced by the use of metakaolin B that is poorly reactive during geopolymerization. Actually, any deviation from leucite composition or inhomogeneities may facilitate the glass formation.[25]

The great linear shrinkage upon heating of the resin and paint obtained from metakaolin B precludes their uses, as the coating dimensional change does not insure a homogeneous and stable protection of the substrates during heat exposure.

The SEM micrographs of Fig. 6 report the cross section and fracture surfaces after thermal treatment at 1300 °C of the coatings realized by brushing SiC-based paints using binders from α-alumina and fumed silica (Fig. 6a and c) or metakaolin A (Fig. 6b). Upon heating, R-SiC grains are embedded into a continuous glassy phase when synthetic raw powders are used, while R-SiC particles are stuck each others when metakaolin A are used as a precursor of the binder. These features are obviously related to the aluminosilicate binder morphology and distribution after setting at 80 °C (Fig. 3). In particular, the geopolymer

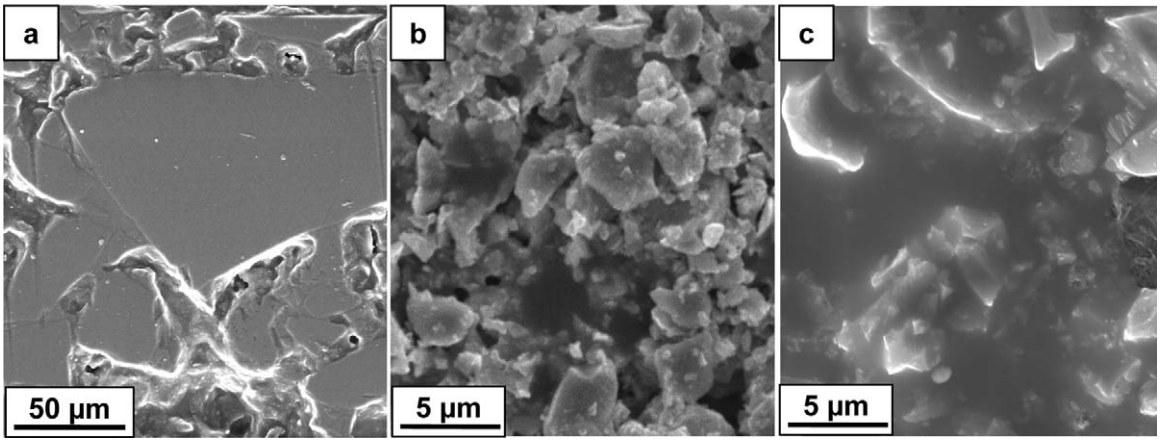

Fig. 6. SEM micrographs showing the microstructure of the polished cross section (a) and of the fracture ((b) and (c)) of the R-SiC-based paints after thermal treatment at 1300 °C for 1 h. The aluminosilicate raw powders are metakaolin A ((a) and (b)) and α-Al_2O_3 plus fumed SiO_2 (c).

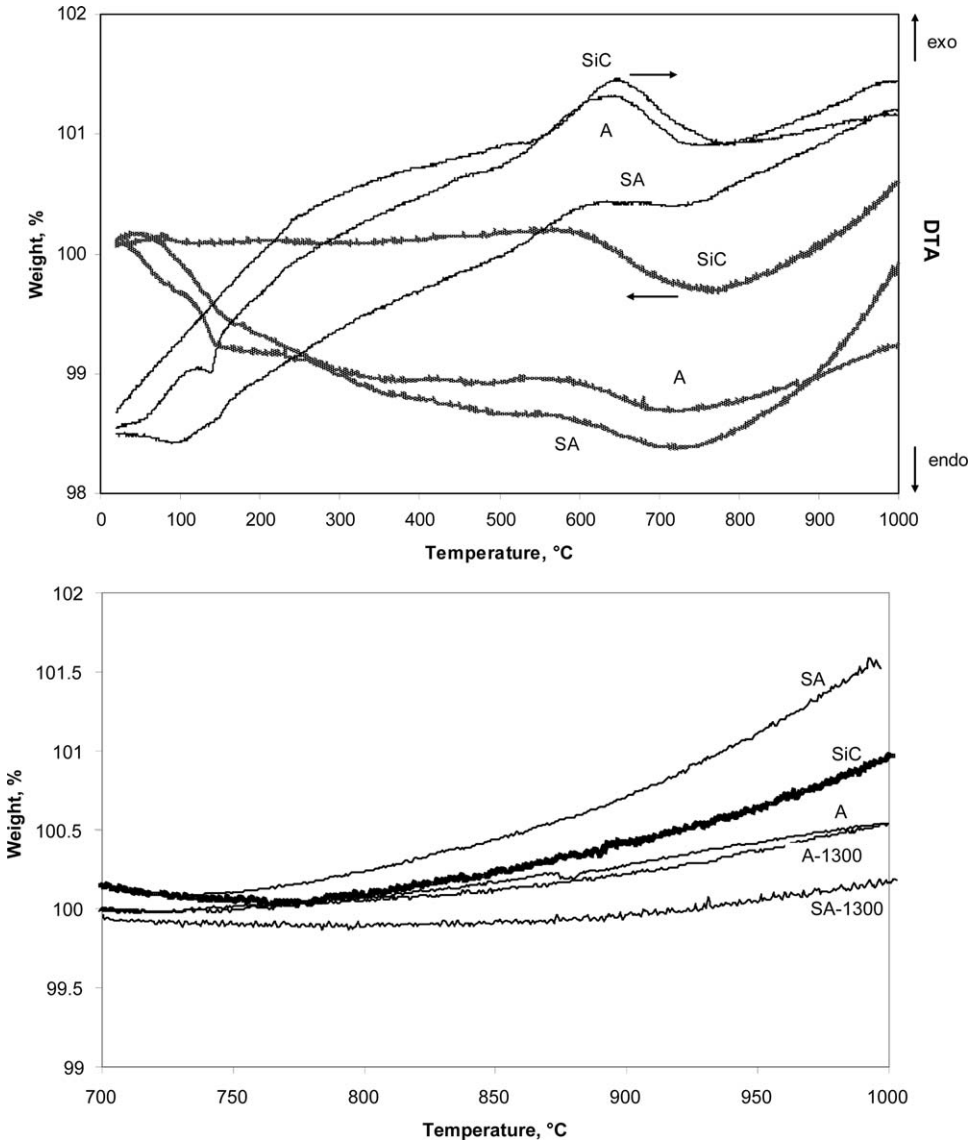

Fig. 7. Non-isothermal simultaneous thermal analyses in air (a) and normalized thermo-gravimetric curves (b) of R-SiC powder and powdered R-SiC-bases paints prepared from different alkali aluminosilicate binders. SA stands for synthetic raw materials, i.e. α-Al_2O_3 plus fumed SiO_2, while 1300 indicates the temperature of a previous thermal treatment in inert atmosphere.

nano-precipitates from metakaolin A melt and form a thin layer that stick the R-SiC particles.

3.3. Oxidation behaviour

Non-isothermal simultaneous thermal analyses in air of R-SiC powder and powdered R-SiC-bases paints prepared from different alkali aluminosilicate binders are reported in Fig. 7. No weight change has been registered for R-SiC up to 600 °C, where a weight loss of 1% may be related to residual carbon combustion, as suggested by the exothermic peak in the DTA analysis. The apparent weight gain due to R-SiC oxidation to form silica and gaseous carbon oxides starts at 780 °C, as reported in Table 3. The R-SiC-based paints cured at 80 °C show a weight loss due to water removal (vaporization), as suggested by the endothermic peak around 130 °C, confirming the dilatometric analyses (Fig. 4). The weight losses at about 600 °C are related to the oxidation of carbon as in R-SiC powder.

Normalized thermo-gravimetric curves in the temperature range 700–1000 °C (Fig. 7b) show different staring oxidation temperatures and oxidation rates (Table 3) as a function of the alkali aluminosilicate binders and thermal treatments.

By using binder from metakaolin A, the stating oxidation temperature is 760 °C, i.e. 20 °C lower than in pure R-SiC, and the oxidation rate is 2.5 °C/min, i.e. 61% of the R-SiC value (or 68% if the 90 wt.% R-SiC composition is considered). The oxidation starts at lower temperature because the silica layer, that is usually present on the R-SiC surface, is leached by the KOH/K_2SiO_3 solution. Moreover, the oxidation rate is slower because it is associated with the weight gain due to the surface oxidation of R-SiC, that is less accessible than pure R-SiC due to an irregular coating of geopolymer nano-precipitates (Fig. 3b). Changes in the oxidation behaviour are not registered when a

Table 3
Oxidation parameters such calculated on simultaneous thermal analysis and long term oxidation at 1200 °C in static air. Paints are indicated by the aluminosilicate raw powders that constitute the binder, while 1300 indicates the thermal treatment at 1300 °C in inert atmosphere before the oxidation tests.

Sample	STA analyses		Long term oxidation	
	Starting oxidation temperature, °C	Oxidation rate (850–1000 °C) 10^{-3} °C/min	Linear shrinkage (%)	SiC oxidation weight gain[a] (%)
Pure SiC	780	4.1	–	13.3
Metakaolin A	760	2.5	0	7.0
Metakaolin A-1300	760	2.5	–	–
α-Al_2O_3; fumed SiO_2	740	6.7	–	–
α-Al_2O_3; fumed SiO_2-1300	850	1.7	0	6.5

[a] The values are calculated considering 90 wt.% R-SiC paints and weight losses due to water removal and carbon oxidation (Fig. 7a).

thermal treatment at 1300 °C in inert atmosphere is performed before the STA analysis.

When fumed SiO_2 and α-Al_2O_3 are used to produce the binder, a thermal treatment at 1300 °C in inert atmosphere results in an improved oxidation resistance. The oxidation rate is lowered from 6.7 to 1.7 × 10^{-3} °C/min, while the staring oxidation temperature increases from 740 °C to 850 °C. This trend may be related to a protective effect of the glassy phase that homogenously surrounds the R-SiC grains (Fig. 6b). It follows that, before the oxidation treatments, the paints prepared using the binder from α-alumina and fumed silica should be "stabilized" by a thermal treatment at 1300 °C in Ar.

After long term oxidation at 1200 °C, the weight gains related to the oxidation of SiC in SiC-based paints are about 50% of the pure R-SiC powder (Table 3), while shrinkages do not occur. Before oxidation, the paints prepared with binder from synthetic raw powders are stabilized in inert atmosphere, as discussed above.

The microstructural features after long term oxidation at 1200 °C of the R-SiC paints applied on Si_3N_4-TiN composite substrate are reported in Figs. 8 and 9. Si_3N_4-TiN composite was chosen because of the linear expansion coefficient similar to that of R-SiC and the well know oxidation behaviour at 1200 °C, that is a limit temperature for the application of this composite.[36,37]

The oxidized surface of the R-SiC paint from metakaolin A is not homogeneous (Fig. 8a and b), since glassy areas are present together with oxidized R-SiC particles. The glassy areas embed facetted rutile grains up to 50 μm in size. The R-SiC paint from

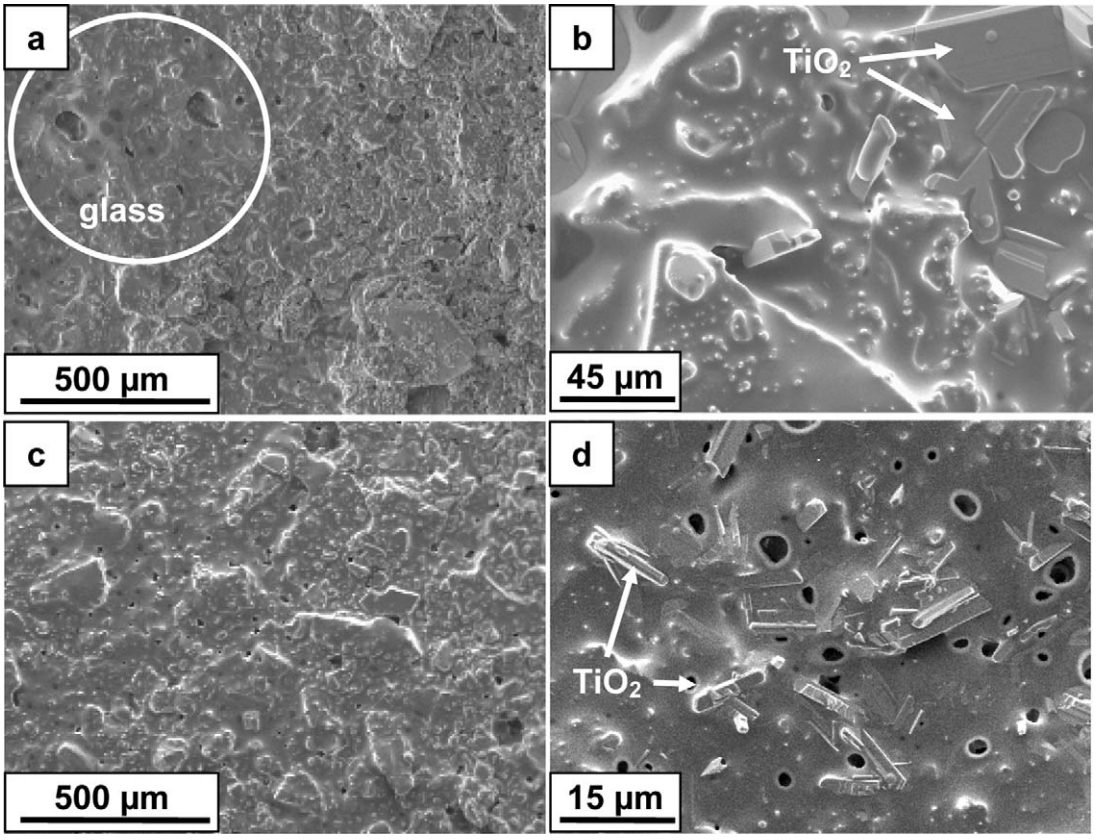

Fig. 8. SEM micrographs showing the surface microstructure of the R-SiC coatings applied on Si_3N_4-TiN composite substrate after long term oxidation tests at 1200 °C. (a) and (b) R-SiC paint with binder from metakaolin A and setting at 80 °C; (c) and (d) R-SiC paint with binder from α-Al_2O_3 plus fumed SiO_2 and thermal treatment at 1300 °C in Ar before oxidation test.

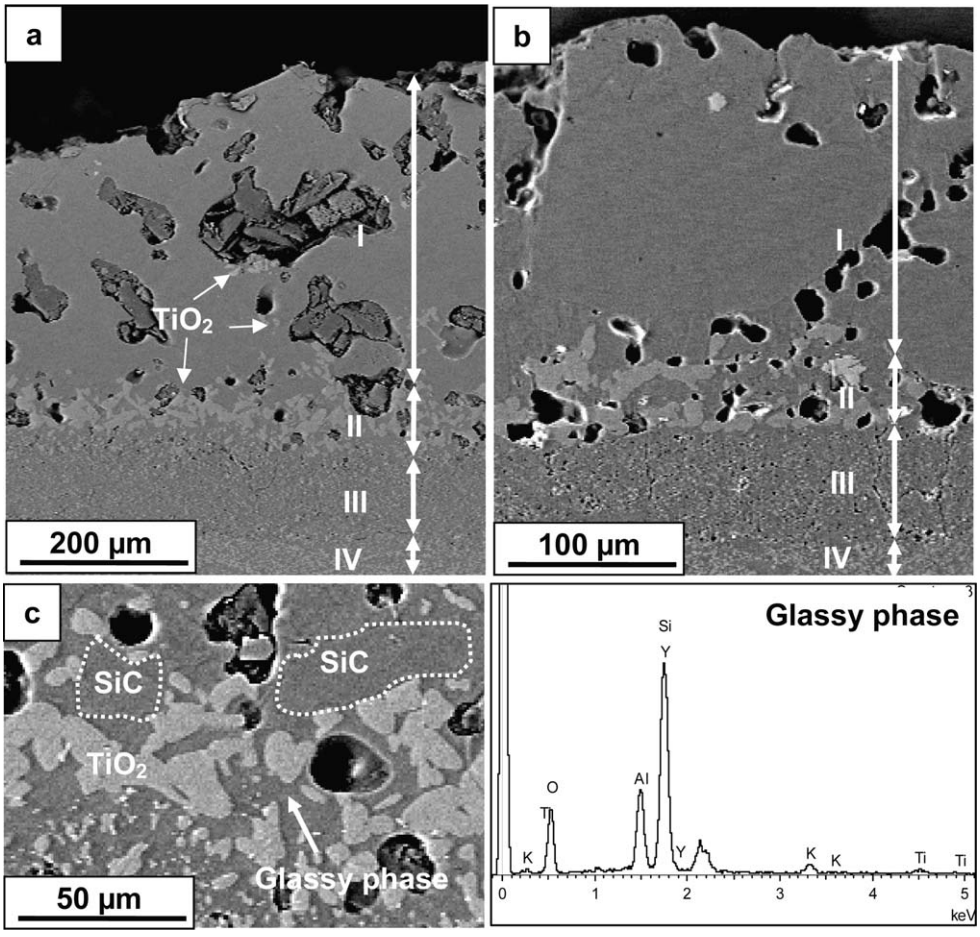

Fig. 9. Back scattered electron micrographs (BSE-SEM) showing the multilayered cross section of the R-SiC coatings applied on the Si_3N_4-TiN substrate after long term oxidation tests at 1200 °C: I – SiC coating; II – oxidized Si_3N_4-TiN layer; III – Si_3N_4-TiN porous sub-layer; IV – Si_3N_4-TiN bulk. (a) and (c) R-SiC paint with binder from metakaolin A and setting at 80 °C: EDS spectrum shows the glassy phase elemental composition in II; (b) SiC paint with binder from α-Al_2O_3 plus fumed SiO_2 and thermal treatment at 1300 °C in Ar before oxidation test.

synthetic raw materials shows a glassy surface with escaping pores of few microns, due to gases evolution through the continuous glassy phase, such as CO_x due to the oxidation of R-SiC and N_2 formed by oxidation of nitrides in the substrate.[36,37] Elongated TiO_2 grains (up to 10 μm) are also observed on the surfaces; the presence of rutile grains suggests that Si_3N_4-TiN composite substrate is partially oxidized, since TiO_2 has been observed in the oxidation of TiN.[36,37]

The microstructural analyses of the mirror polished cross sections (Fig. 9) confirms that although the R-SiC coatings are well adherent to the substrates (they survived the cutting and polishing operations of the cross sections), the Si_3N_4-TiN substrate is oxidized. It is noteworthy that R-SiC coatings are macroporous, due to the non optimal R-SiC particle distribution within the paints. The macroporosity offers an easy access to O_2 and the oxidation resistance should benefit of its reduction. Moreover, as the coatings are manually applied by brushing, the thicknesses may vary between 200 and 300 μm. However, the trend established by STA analyses (Table 3 and Fig. 7) is confirmed by long term oxidation tests at 1200 °C.

The cross sections appear multilayered, because of the formation of two layers between the R-SiC coating and the Si_3N_4-TiN bulk material, as well evidenced in Fig. 9: the former may be described as an oxidized Si_3N_4-TiN layer, i.e. it is mainly formed by the oxidation products of the substrate, and it is placed just below the R-SiC coating; the latter is a porous sub-layer situated just above the unreacted Si_3N_4-TiN bulk substrate. This porous sub-layer is the consequence of the migration of TiN particles that undergo oxidation and migrate within the glassy phase toward the surface.[36,37]

By using binder from metakaolin A and a simple setting at 80 °C, an oxidized Si_3N_4-TiN layer ranging between 60 and 80 μm appears below the R-SiC coating (Fig. 9a and c). EDS analysis evidences that this layer is mainly composed by rutile grains and silicatic glassy phase with Y- and Al-traces from the sintering aids used to promote the complete densification of the substrate[36] and K-traces from alkaline alluminosilicatic binder. The diffusion and reprecipitation of rutile occur both on the surface and within the R-SiC coating because of the formation of a glassy phase that allows cations and oxygen counter-diffusion. The real reaction interface of the Si_3N_4-TiN composite is not clearly identified because of the presence of a 70 μm thick porous sub-layer between the oxidized layer and the bulk material.

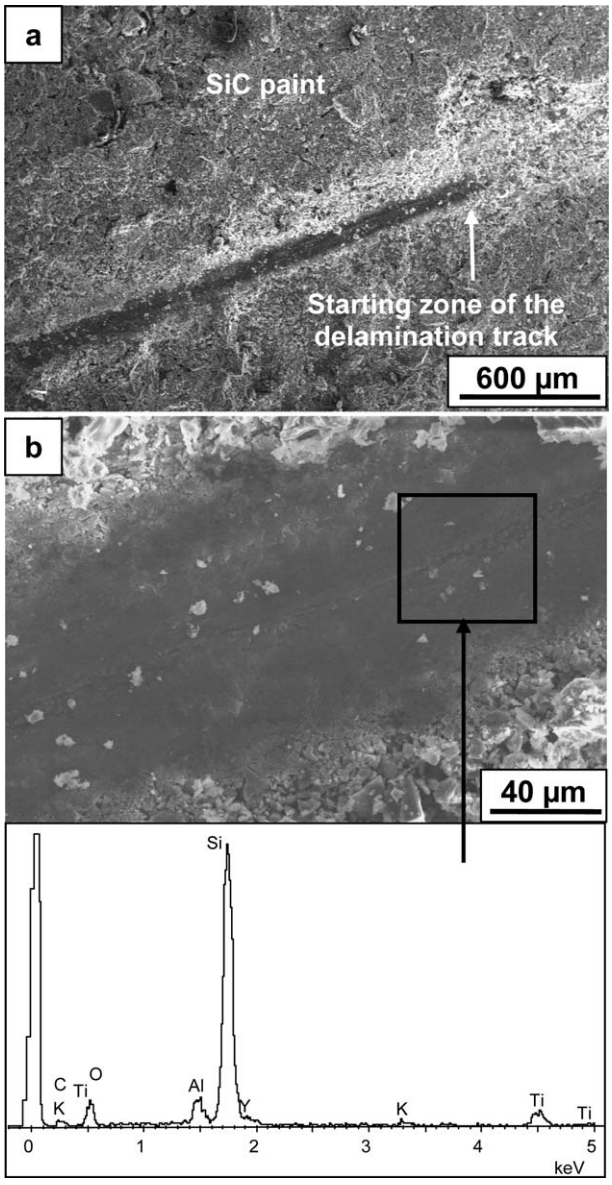

Fig. 10. SEM micrographs showing the delamination track after scratch tests performed on R-SiC paint with binder from metakaolin A and setting at 80 °C. (b) Starting zone of the delamination track and EDS spectrum confirming the exposition of the Si_3N_4-TiN substrate.

For comparison, by using α-alumina and fumed silica as raw powders for the alkali aluminosilicate binder and a thermal treatment at 1300 °C in inert atmosphere before oxidation, a oxidized layer ranging between 30 and 60 μm appears below the R-SiC coating and the diffusion of Ti (to form rutile on the surface) and other cations was scarce, while the porous sub-layer is 50 μm thick.

3.4. Adhesion resistance

A first indication of the good adhesion resistance of the SiC coatings is the absence of exfoliation or detaching upon cutting and polishing of the cross sections before and after long term oxidation.

Scratch tests were performed on R-SiC paint using binder from metakaolin A. After setting at 80 °C, cracks due to scarce adhesion do not appear on the substrate, while coating delamination starts at about 30 N (Fig. 10a). The EDS analysis on the starting zone of the delamination track confirms the Si_3N_4-TiN substrate material exposition, showing the presence of Ti peak from TiN phase (Fig. 10b).

After long term oxidation at 1200 °C, no clear coating delamination is observed: the glassy phase formation and interdiffusion during oxidation allow a tight adhesion between the coating and the substrate.

4. Conclusions

In this feasibility study, R-SiC refractory coatings have been showed to perform as easy-to-prepare and easy-to-apply paints.

Alkali aluminosilicates inorganic binders are used to withstand high working temperatures. The binders may be prepared by using metakaolins or α-alumina and fumed silica as raw powders, and a KOH/K_2SiO_3 aqueous solution. On the base of their reactivity in the alkaline solution, metakaolins form geopolymer precipitates that act as a glue for R-SiC particle. Binder from synthetic raw materials (α-alumina and fumed silica) behaves as water glass (potassium silicate solution).

A key role of the alkali aluminosilicate binders on paints thermal stability is evidenced. R-SiC paints, having minimal shrinkage upon heating, have been successfully prepared using binder from highly reactive metakaolins. Moreover, the preliminary oxidation tests evidence the good oxidation resistance of the paints already after curing at 80 °C. R-SiC coatings applied by brushing on Si_3N_4-TiN substrate were not optimized as a barrier against oxygen penetration due to the presence of large pores. However, this new type of refractory material exhibits potential for further improvements by the optimization of the R-SiC granulometric distribution which should reduce the residual porosity. Good adhesion of the paints on the substrate has been evidenced by preliminary scratch tests and the absence of exfoliation or detaching upon cutting and polishing of the cross section. The developed SiC paint may be suitable to protect the substrate from erosion and/or cavitation at operating high temperature conditions. Moreover, if the R-SiC protective coating is damaged during the activity, the repair by a simple paint brushing may be hypothesized.

Acknowledgement

Thanks are due to Dr. Maria Giulia Faga for the scratch tests and the useful discussions on the adhesion resistance.

References

1. Tsou HT, Kowbel W. A hybrid PACVD multilayer coating for oxidation protection of composites. *Carbon* 1995;**33**(9):1279–88.
2. Angelelis C, Ducarroir M, Felder E, Ignat M, Scordo S. Mechanical testing by bending, nano- and macro-indentation of micro-wave PACVD SiC coatings on steel. *Annales de Chimie Science des Materiaux* 1998;**23**(5–6):891–8.

3. Rivière JP, Zaytouni M, Delafond J. Characterization and wear behavior of SiC coatings prepared by ion beam assisted deposition. *Surface and Coatings Technology* 1996;**84**(1–3):376–82.
4. Uma Devi M. On the nature of phases in Al_2O_3 and Al_2O_3–SiC thermal spray coatings. *Ceramics International* 2004;**30**(4):545–53.
5. Jiansirisomboon S, MacKenzie KJD, Roberts SG, Grant PS. Low pressure plasma-sprayed Al_2O_3 and Al_2O_3/SiC nanocomposite coatings from different feedstock powders. *Journal of the European Ceramic Society* 2003;**23**(6):961–76.
6. Yerokhin AL, Nie X, Leyland A, Matthews A, Dowey SJ. Plasma electrolysis for surface engineering. *Surface and Coatings Technology* 1999;**122**(2–3):73–93.
7. Chen D, He L, Shang S. Study on aluminum phosphate binder and related Al_2O_3–SiC ceramic coating. *Materials Science and Engineering A* 2003;**348**(1–2):29–35.
8. Davidovits J. 30 years of successes and failures in geopolymer applications. Market trends and potential breakthroughs. In: Lukey G, editor. *Proceedings of geopolymer 2002 3rd international conference*. 2002. p. 1–16.
9. Davidovits J. Geopolymers: inorganic polymeric new materials. *Journal of Thermal Analysis* 1991;**37**:1633–56.
10. Gordon M, Bell J, Kriven WM. Geopolymers: alkali bonded ceramics (ABCs) for high-tech applications. *Ceramic Transaction* 2006;**175**:215–24.
11. Kriven WM, Bell JL, Gordon M. Microstructure and microchemistry of fully-reacted geopolymers and geopolymer matrix composites. *Ceramic Transactions* 2003;**153**:227.
12. Bortnovsky O, Dedeček J, Tvarůžková Z, Sobalík Z, Šubrt J. Metal ions as probes for characterization of geopolymer materials. *Journal of the American Ceramic Society* 2008;**91**:3052–7.
13. Kriven WM, Gordon M, Bell J, Geopolymers:. Nanoparticulate, nanoporous ceramics made under ambient conditions. In: Anderson IM, Price R, Hall E, Clark E, McKernan S, editors. *Proceedings of the 62nd annual meeting of microscopy society of America*. 2004. p. 404–5, vol. 10.
14. Buchwald A, Vicent M, Kriegel R, Kaps C, Monzó M, Barba A. Geopolymeric binders with different fine fillers – phase transformations at high temperatures. *Applied Clay Science* 2009;**46**:190–5.
15. Comrie DC, Kriven WM. Composite cold ceramic geopolymer in a refractory application. *Ceramic Transactions* 2003;**153**:211–25.
16. Zhao Q, Nair B, Rahimian T, Balaguru P. Novel geopolymer based composites with enhanced ductility. *Journal of Materials Science* 2007;**42**:3131–7.
17. Zhang Y, Sun W, Li Z, Zhou X, Eddie, Chau C. Impact properties of geopolymer based extrudates incorporated with fly ash and PVA short fiber. *Construction and Building Materials* 2008;**22**:370–83.
18. Lin TS, Jia DC, He PG, Wang MR, Liang D. Effects of fiber length on mechanical properties and fracture behaviour of short carbon fiber reinforced geopolymer matrix composites. *Materials Science and Engineering A* 2008;**497**:181–5.
19. Lin TS, Jia DC, He PG, Wang MR. Thermo-mechanical and microstructural characterization of geopolymers with alpha-Al_2O_3 particle filler. *International Journal of Thermophysics* 2009;**30**:1568–77.
20. Provis JL, Yong CZ, Duxson P, van Deventer JSJ. Correlating mechanical and thermal properties of sodium silicate-fly ash geopolymers. *Colloids and Surfaces A: Physicochemical and Engineering Aspects* 2009;**336**:57–63.
21. Pernica D, Reis PNB, Ferreira JAM, Louda P. Effect of test conditions on the bending strength of a geopolymer-reinforced composite. *Journal of Materials Science* 2010;**45**:744–9.
22. He PG, Jia DC, Wang MR, Zhou Y. Improvement of high-temperature mechanical properties of heat treated Cf/geopolymer composites by Sol-SiO_2 impregnation. *Journal of the European Ceramic Society* 2010;**30**:3053–61.
23. Panagiotopoulou Ch, Kontori E, Perraki Th, Kakali G. Dissolution of aluminosilicate minerals and by-products in alkaline media. *Journal of Material Science* 2007;**42**:2967.
24. Bell JL, Driemeyer PE, Kriven WM. Formation of ceramics from metakaolin based geopolymers: part I – Cs-based geopolymer. *Journal of the American Ceramic Society* 2009;**92**(1):1–8.
25. Bell JL, Driemeyer PE, Kriven WM. Formation of ceramics from metakaolin-based geopolymers. Part II: K-based geopolymer. *Journal of the American Ceramic Society* 2009;**92**(3):607–15.
26. http://nmr.cemhti.cnrs-orleans.fr/dmfit/.
27. Steinmann PA, Tardy Y, Hintermann HE. Adhesion testing by the scratch test method: the influence of intrinsic and extrinsic parameters on the critical load. *Thin Solid Films* 1987;**154**:333–49.
28. Medri V, Fabbri S, Dedecek J, Sobalik Z, Tvaruzkova Z, Vaccari A. Role of the morphology and the dehydroxylation of metakaolins on geopolymerization. *Applied Clay Science* 2010;**50**:538–45.
29. Davidovits J. *Geopolymers chemistry and applications*. 3rd ed. Saint-Quentin: Institute Geopolymere; 2008.
30. Zibouche F, Kerdjoudj H, d'Espinose de Lacaillerie J-B, Van Damme H. Geopolymers from Algerian metakaolin. Influence of secondary minerals. *Applied Clay Science* 2009;**43**:453.
31. MacKenzie KJD, Smith ME. *Multinuclear solid-state NMR of inorganic materials*. Amsterdam: Pergamon; 2002.
32. Wang MR, Jia DC, He PG, Lin TS, Zhou Y. Influence of calcinations temperature of kaolin on the structure and properties of the final geopolymer. *Materials Letters* 2010;**64**:2551–4.
33. Munro RG. Material properties of a sintered α-SiC. *Journal of Physical and Chemical Reference Data* 1997;**26**(5):1195–203.
34. Mackert JR, Evans AL. Quantitative X-ray-diffraction determination of leucite thermal-instability in dental porcelain. *Journal of the American Ceramic Society* 1991;**74**:450–3.
35. Kingery WD, Bowden HK, Uhlmann DR. *Introduction to ceramics*. 2nd ed. New York: Wiley; 1976.
36. Klein R, Medri V, Desmaison-Brut M, Bellosi A, Desmaison J. Influence of additives content on the high temperature oxidation of silicon nitride based composites. *Journal of the European Ceramic Society* 2003;**23**: 603–11.
37. Bracisiewicz M, Medri V, Bellosi A. Factors inducing degradation of properties after long term oxidation of Si_3N_4-TiN electroconductive composites. *Applied Surface Science* 2002;**202**:139–49.